

Spatial integral projection models predict slow
creosotebush encroachment between episodes of rapid
expansion

Trevor Drees^{*a,b}, Brad M. Ochocki^b, Scott L. Collins^c, and Tom E.X. Miller^b

^aDepartment of Biology, Penn State University, State College, PA USA

^bProgram in Ecology and Evolutionary Biology, Department of BioSciences, Rice
University, Houston, TX USA

^cDepartment of Biology, University of New Mexico, Albuquerque, NM USA

September 3, 2020

^{*}thd5066@psu.edu

1 Abstract

2 **Encroachment**¹ of shrubs into adjacent grasslands has become an increasingly reported
3 phenomenon across the world, and such encroachment is either pulled forward by high
4 population growth at the low-density encroachment front or pushed forward by higher-
5 density areas behind the front. However, at sites such as Sevilleta National Wildlife
6 Refuge in central New Mexico, little is known about whether encroachment is pushed or
7 pulled, and the dynamics of encroachment are not well-understood. Here, long-term en-
8 croachment of creosotebush (*Larrea tridentata*), a native perennial shrub, stands in stark
9 contrast with the stagnation in encroachment observed in recent decades. In order to
10 better understand creosotebush encroachment at this site, we quantify it using a spatially
11 structured population model where a wave of individuals travels at a speed governed by
12 both dispersal and density-dependence. Results indicate that population growth rates
13 generally increase with decreasing density, suggesting that encroachment is pulled by
14 individuals at the low-density wave front, and the spatial population model predicts an
15 encroachment rate of less than 2 cm per year. While the predicted rate of encroach-
16 ment is consistent with observations over recent decades, it does not explain long-term
17 creosotebush encroachment at the study site, suggesting that this process may occur in
18 pulses when recruitment, seedling survival, or dispersal significantly exceed typical rates.
19 Overall, our work demonstrates that individuals at low densities are likely the biggest
20 contributors to creosotebush encroachment at this site, and that this encroachment is
21 likely a process that occurs in large but infrequent bursts rather than at a steady pace.

22 Keywords

23 density-dependence, ecotones, woody encroachment, shrubs, integral projection model,
24 grassland

¹*I am not editing the abstract for now.*

25 Introduction

26 The encroachment of shrubs and other woody plants into adjacent grasslands has caused
27 significant vegetation and landscape changes in ecosystems where this process takes place,
28 and as such has become the focus of an increasing number of studies in recent years.
29 This process of encroachment generally involves **increases in number and/or density**² of
30 woody shrub-like plants in a given area (Van Auken, 2000), which can displace other
31 species and alter abiotic aspects of the local ecosystem. Woody plant encroachment has
32 been observed across many arid and semi-arid regions, such as the grasslands of the
33 southwestern United States (Van Auken, 2000, 2009; Goslee et al., 2003; Gibbens et al.,
34 2005) and southern South America (Parizek et al., 2002; Cabral et al., 2003), savannas
35 of southern Africa (Trollope et al., 1989; Roques et al., 2001), and Asian steppes (Peng
36 et al., 2013; Chen et al., 2015). Such encroachment may involve native or invasive plants
37 and can adversely affect ecosystems in which it occurs, as the resulting increases in shrub
38 biomass and density are considered to be strong drivers of ecosystem degradation and/or
39 desertification (Schlesinger et al., 1990; Ravi et al., 2009) due to how these plants alter
40 the distribution of soil resources (Schlesinger and Pilmanis, 1998; Knapp et al., 2008).
41 Other adverse effects of encroachment include changes in ecosystem services (Reed et al.,
42 2015; Kelleway et al., 2017), declines in biodiversity (Ratajczak et al., 2012; Sirami and
43 Monadjem, 2012; Brandt et al., 2013), and economic losses in areas where the proliferation
44 of shrubs adversely affects grazing land and pastoral production (Mugasi et al., 2000; Oba
45 et al., 2000).³

46 The encroachment of woody plants into adjacent grasslands involves the movement
47 of shrub-grass ecotones where a population of individuals is a gradient of conspecific
48 density, and propagates as a wave across space and over time (Kot et al., 1996; Neubert

²*this description misses the spatial aspect*

³*I think it would be good for this first paragraph to introduce the idea of habitat ecotones, the need to understand whether these are stable, and how they may respond to global change drivers. You can then introduce woody encroachment as a specific and widespread type of ecotone.*

49 and Caswell, 2000; Wang et al., 2002; Pan and Lin, 2012). The movement of these waves
50 is largely dependent upon two processes: local demography and dispersal of propag-
51 ules. First, demographic processes affect how populations expand since survival, growth,
52 reproduction, and recruitment rates in the parent plant ultimately affect the number
53 of propagules produced and their fate after release, which is important because these
54 propagules are the very basis for population growth. Second, movement is driven by the
55 spatial dispersal of propagules produced by parent plants, and dispersal plays a role in
56 where the new recruits that drive the wave’s movement are likely to be found. The speed
57 at which expansion waves move is highly dependent upon the shape of the dispersal ker-
58 nel, or the probability distribution of dispersal distances, and is strongly influenced by
59 the frequency of long-distance dispersal events at the tail of the distribution (Skarpaas
60 and Shea, 2007). Additionally, both demography and dispersal are affected by population
61 structure based on age, size, or life stage, which can strongly influence how waves move
62 (Neubert and Caswell, 2000). For example, the reproductive aspect of demography in
63 some plants is affected by age and size, as older individuals may be more likely to repro-
64 duce than younger individuals (Hanzawa and Kalisz, 1993) and larger individuals may
65 reproduce more than smaller individuals (PICKERING, 1994; Smith et al., 2003). This
66 means that within a population of plants, it is possible for the older or taller subset of
67 the population to contribute disproportionately to the next generation. When it comes
68 to dispersal, height influences dispersal via gravity or wind (Nathan et al., 2011) and the
69 propagules of taller plants may travel further than those of their shorter counterparts,
70 possibly making the taller individuals influential contributors to the spatial expansion a
71 the population.

72 Given that expansion waves typically correspond to gradients of conspecific density,
73 the effects of density dependence on demographic rates and population growth are im-
74 portant to consider. Conspecific density affects plants through intraspecific competition
75 for resources: not only does density influence how plants survive, grow, and reproduce,

but it may also determine whether dispersed propagules germinate or are prevented from establishing. Since intraspecific competition governs the performance of individuals within the population, the location of the individuals most responsible for population wave movement is strongly tied to how demographic rates and population growth vary with changes in conspecific density. If population growth has a negative and monotonic relationship with density such that highest rates of population growth tend to be found at the lowest densities, then the invading wave is pulled forward by the plants at the low-density vanguard (Kot et al., 1996). However, if Allee effects result in reduced fitness at low densities⁴, then the wave is instead pushed forward by the individuals behind the front edge (Kot et al., 1996; Taylor and Hastings, 2005; Sullivan et al., 2017). Such Allee effects can greatly limit population growth at the front of the wave, slowing⁵ or halting its movement (Lewis and Kareiva, 1993; Veit and Lewis, 1996; Keitt et al., 2001).

6

In this study, we use data from an ecosystem in which woody encroachment occurs to link the encroachment process to ecological theory for invasion waves, with the goal of better understanding how demographic processes and dispersal drive this encroachment, and determining whether a particular instance of woody encroachment is pushed or pulled. The woody encroachment modelled here comes from study sites in the Chihuahuan Desert of the southwestern United States, where extensive documentation of shrub encroachment exists but little is known about the dispersal and demographic processes that govern it. In areas such as New Mexico, populations of the creosotebush (*Larrea tridentata*) have been expanding into nearby grasslands for approximately 150

⁴*I think this needs to be unpacked a bit more, explaining why fitness may be reduced at low density.*

⁵*I think it would help to have a more explicit statement that, all else equal, a pushed wave should be slower than a pulled wave – I think this is true but we should check and cite, obviously. See two nice references that I will email.*

⁶*I think there should be a new paragraph here that connects the pulled/pushed ideas to shrub encroachment. There is a lot of literature on woody plants being ecosystem engineers. While these are not typically called ‘Allee effects’, you can make the link that we might expect positive density dependence at the leading edge of woody ecotones, and this could slow or halt their expansion. I think this will be an important addition for building your story.*

98 years and have decreased the cover of grasses such as *Bouteloua eriopoda* (Gardner, 1951;
 99 Buffington and Herbel, 1965; Gibbens et al., 2005). This encroachment leads to ecotones
 100 marking a transition from dense shrubland with numerous dry patches to open grassland,
 101 with a transition zone in between where shrubs can often be found interspersed among
 102 their grassy competitors. Historically, long-term creosotebush encroachment into grass-
 103 lands is believed to have been driven by a combination of factors including overgrazing,
 104 drought and variability in rainfall, and suppression of fire regimes Moreno-de las Heras
 105 et al. (2016). These shrubs are also thought to further facilitate their own encroachment
 106 through positive feedback (Grover and Musick, 1990; D’Odorico et al., 2012) by modify-
 107 ing various abiotic aspects of their local environment that **could favour continued growth**
 108 **and dispersal**⁷, such as local climate (D’Odorico et al., 2010) and rates of soil erosion
 109 (Turnbull et al., 2010). Such positive feedback also occurs as herbaceous competitors are
 110 eliminated, reducing competition as well as the amount of flammable biomass used to
 111 fuel the fires that keep creosotebush growth in check (Van Auken, 2000). The existence
 112 of positive feedback mechanisms where creosotebush is present suggests that a lack of
 113 conspecifics at the low-density front of encroachment may depress population growth and
 114 be indicative of an Allee effect, though this has not yet been demonstrated.

115 While there is considerable interest in creosotebush encroachment, literature investi-
 116 gating the dispersal mechanisms and demographic processes that govern this process is
 117 extremely limited, and no previous studies have evaluated demography and dispersal to
 118 understand and predict creosotebush expansion dynamics. We have little understand-
 119 ing of how dispersal, density-dependent demography, and density-dependent population
 120 growth facilitate creosotebush encroachment, as well as a dearth of data regarding popu-
 121 lation dynamics at the vanguard of expanding creosotebush populations. Without better
 122 knowledge on all of these, it becomes rather difficult to model creosotebush encroach-
 123 ment, as doing so requires knowledge of the mechanisms occurring at these grass-shrub

⁷ *Again, I would connect this back to Allee effects/pushed waves, since it suggests that seeds that recruit into high grass densities at the leading edge should suffer from lack of conspecifics.*

boundaries. Such gaps in knowledge make it difficult to make estimates of encroachment rates that extend beyond what can be gathered from vegetation surveys.

Our investigations are novel in the sense that they will be some of the first to apply a wave model of population expansion to ecotones of *Larrea tridentata* and its grassy competitors, using density-dependent demographic rates and recruitment to describe the dynamics of ecotone movement in this specific system. This research aims to fill the aforementioned knowledge gaps by not only collecting data on demographic rates and dispersal in *Larrea tridentata*, but by examining creosotebush encroachment in the framework of a wave model; by examining this system in such a way we can estimate the rate of creosotebush encroachment, and additionally determine whether this encroachment is pulled by the low-density wavefront pushed by high-density areas behind the wavefront. As such, we address the following questions: 1) What is the observed rate of creosotebush encroachment in recent past? 2) How do creosotebush size and conspecific density affect demographic rates such as growth and reproduction? 3) What does the dispersal kernel for this species look like and how far do propagules typically travel? 4) Using a wave model, what is the estimated rate of encroachment, and does it differ from the observed rate? and 5) Is the encroachment pulled by the individuals at the front of the wave or instead pushed by the individuals behind it? To answer these questions, we use a spatial integral projection model that combines dispersal data with demography data from surveys and transplant experiments.

Materials and methods

Study system

Paragraph about creosotebush at the SEV. [WIP] Creosotebush is a woody perennial native that is extremely drought-resistant and has a typical lifespan of # years. These shrubs are extremely efficient at absorbing water from the soil and tend to create large patches

149 *of barren soil where nothing else can grow. Creosotebush reproduces both asexually and*
150 *sexually. Shrubs can contain numerous small, yellow flowers that eventually give rise to*
151 *highly pubescent seeds. Seeds are dispersed from the parent plant by gravity and wind, and*
152 *can experience secondary dispersal by kangaroo rats. Here, we examine the encroachment*
153 *of creosotebush at the Sevilleta National Wildlife Refuge in central New Mexico. This*
154 *area receives approximately # of rainfall per yea andr consists of lowland shrub-grass*
155 *ecotones as well as mountainous areas with juniper and pinon pine. While there is a*
156 *history of creosotebush encroachment at the SEV, it seems to have stagnated over the*
157 *past few decades; the reasons for this are largely unknown.*

158 **Encroachment re-surveys**

159 We recorded shrub percent cover along two permanent 1000-m transects that spanned
160 the shrub-grass ecotone, from high to low to near-zero shrub density. These surveys were
161 conducted in summer 2001 and again in summer 2013 to document change in the spatial
162 extent of shrub encroachment. At every 10 meters, shrub cover was recorded in nine
163 cover classes (<1%, 1–4%, 5–10%, 10–25%, 25–33%, 33–50%, 50–75%, 75–95%, >95%).
164 For analysis, we visually assessed midpoint values of these cover classes at each meter
165 location for both transects and years.

166 **Annual censuses**

167 **Demographic data collection**

168 Collection of creosotebush demographic data occurred during the early summer of every
169 year from 2013-2017, at the Sevilleta National Wildlife Refuge LTER site in central New
170 Mexico. Four different sampling sites in the eastern part of the reserve were designated,
171 with each of the sites containing 3 different transects. Lengths of these transects varied
172 from 200 to 600 m, and no two sites had identical compositions of transect lengths.
173 Transect length was determined by the strength of vegetation transition, as areas where

174 shrubland more quickly transitions to grassland do not need as long of a transect to
175 capture the gradient of densities as a more gradual transition does. All transects were
176 placed longitudinally along the shrubland-grassland ecotone so a full range of shrub
177 densities could be captured; each transect spanned shrub-dense "core" areas as well as
178 grasslands with few shrubs and the transition zones in between.

179 Only plants within a metre of the transect on either side were considered when de-
180 termining baseline shrub densities. These densities were calculated using initial mea-
181 surements from 2013 and were assumed to remain relatively static over the course of
182 the study; each density was recorded as the weighted total amount of shrub volume per
183 5-m transect subsection. The per-shrub volume was calculated as that of an elliptic
184 cone, as this was found to be the figure most closely matching the plant's morphology,
185 using the formula $V_i = \pi lwh/3$ where l , w , and h are the maximum length, maximum
186 width, and height, respectively. Maximum length and width were measured so that they
187 were always perpendicular to each other, and height was measured from the base of
188 the woody stem at the soil surface to the highest part of the shrub. All three of these
189 dimensional measurements were mutually orthogonal and were inclusive only of living
190 parts of the shrub; dead wood and non-foliated outer sections were not included in mea-
191 surements. The total weighted density for the window was then expressed as the sum
192 of log-transformed volumes of each individual shrub contained within. Such a weighted
193 density was chosen because density of individuals alone can often fail to be a useful mea-
194 surement in environments where large size differences between plants of the same species
195 exist. Different-sized plants may vary greatly in their ability to extract resources from the
196 environment around them and may thus differ greatly in their degree of competitiveness
197 (Weiner, 1990; HARA, 1993). By using a weighted density in terms of shrub volume,
198 we were able to account for the extra competitiveness of larger shrubs and thus have
199 a more accurate measurement of conspecific presence that is more suitable for a study
200 population containing significant heterogeneity in size.

201 A subset of the shrubs used to calculate the baseline densities were tagged, with each
202 plant given a unique identifier that allowed it to be recognised based on sampling site,
203 transect number, and location within 50-m and 5-m subsections. These tagged shrubs
204 then had various demographic measurements recorded on an annual basis. Maximum
205 width, length, and height on each shrub were measured in order to calculate conical
206 volume, using the formula given earlier. Survival status of the shrubs was also recorded,
207 with dead individuals being noted and excluded from measurements in subsequent years.
208 Counts of flowers and fruits on each shrub were recorded as well. In instances where
209 shrubs had large numbers of reproductive structures that would prove difficult to reliably
210 count, estimates were made, with a more accurate count on a fraction of the shrub being
211 extrapolated to the entire individual. The position of each shrub along the transect was
212 noted to a resolution of 5 m so that it could be matched with the baseline density of its
213 corresponding subsection. For shrubs in which a given 5-m subsection was not recorded,
214 their position was estimated to the nearest 50 m; however, compared to the number of
215 finer-resolution 5-m subsections, this occurred relatively infrequently. Establishment of
216 recruits was also accounted for, with new recruits observed within the study area tagged
217 and measured.

218 **Demographic data analysis**

219 Collected demography data were then examined to investigate how weighted density
220 and shrub volume affected four different demographic variables: survival, probability
221 of flowering (i.e. producing at least one flower or fruit), annual growth, and number of
222 reproductive structures. Each of these demographic variables was fit to a different mixed-
223 effects model through maximum likelihood. Both survival and probability of flowering
224 were each fit to generalised linear mixed-effects models using a binomial response and a
225 logit link function. Annual growth was defined as $\ln(V_{t+1}/V_t)$ where V_{t+1} and V_t are the
226 shrub volumes in the current and previous years, respectively, and was then fit to a linear

227 mixed-effects model. The number of reproductive structures was defined as the natural
 228 logarithm of the sum of fruits and flowers on the entire shrub and was fit to a linear
 229 mixed-effects model as well. To construct these models, all of the equations listed in
 230 Table 1 were first fit to each of the four demographic variables, with each equation using
 231 volume and standardised density as predictors while also treating the unique transect
 232 in which each shrub was located as a random effect. After these equations were fit to
 233 the data, all eight equations for each demographic variable were ranked based on their
 234 value of the Akaike information criterion (AIC) and weighted based on their quality so
 235 that better-fitting models had a higher weight. Then, coefficients of the same type were
 236 averaged between all eight models for each demographic variable using a weighted mean
 237 corresponding to model quality in order to generate an average model. All four average
 238 models have the general form

$$239 \quad R = \beta_1 v + \beta_2 d + \beta_3 d^2 + \beta_4 v d + \beta_5 v d^2 + \epsilon \quad (1)$$

240 where R is the response variable, v and d are the volume and density, ϵ is a random
 241 transect effect, and β is the coefficient for each type of term.

242 The effect of density dependence on the probability of recruitment from seeds was
 243 also modelled. For every year, the sum of seeds produced the prior year was calculated
 244 for each 5-m subsection, and then probability of recruitment was calculated as the num-
 245 ber of recruits observed in each 5-m subsection divided by that number of seeds. For
 246 any subsection in which seeds were not found, a count of seeds was estimated based on
 247 the number of seeds in a subsection of similar weighted density; this was done to avoid
 248 creating any undefined values of recruitment probability. Both linear and quadratic mod-
 249 els using only weighted density as a predictor were fit to the distribution of recruitment
 250 probabilities, though the linear model was ultimately used because it had a higher AIC
 251 value.

252 **Transplant experiment**

253 **Transplant data collection**

254 **Transplant data analysis**

255 **Dispersal modelling**

256 Dispersal kernels were calculated using the WALD, or Wald analytical long-distance
257 dispersal, model that uses a mechanistic approach to predict dispersal patterns of plant
258 propagules by wind. The WALD model, which is largely based in fluid dynamics, can
259 serve as a good approximation of empirically-determined dispersal kernels (Katul et al.,
260 2005; Skarpaas and Shea, 2007) and may be used when empirical dispersal data is not
261 readily available. Under the assumptions that wind turbulence is low, wind flow is
262 vertically homogenous, and terminal velocity is achieved immediately upon seed release,
263 the WALD model simplifies a Lagrangian stochastic model to create a dispersal kernel
264 that estimates the likelihood a propagule will travel a given distance (Katul et al., 2005).
265 This dispersal kernel takes the form of the inverse Gaussian distribution

$$266 \quad p(r) = \left(\frac{\lambda'}{2\pi r^3} \right)^{\frac{1}{2}} \exp \left[-\frac{\lambda'(r - \mu')^2}{2\mu'^2 r} \right] \quad (2)$$

267 that is a slight adaptation from equation 5b in Katul et al. (2005), using r to denote
268 dispersal distance. Here, λ' is the location parameter and μ' is the scale parameter,
269 which depend on environmental and plant-specific properties of the study system. The
270 location and scale parameters are defined as $\lambda' = (H/\sigma)^2$ and $\mu' = HU/F$; these are
271 functions of the height H of seed release, wind speed U at seed release height, seed
272 terminal velocity F , and the turbulent flow parameter σ that depends on both wind
273 speed and local vegetation roughness.

274 In order to create the dispersal kernel, we first take the wind speeds at measure-
275 ment height z_m and correct them to find wind speed U for any height H by using the

276 logarithmic wind profile

$$277 \quad U = \frac{1}{H} \int_{d+z_0}^H \frac{u^*}{K} \log \left(\frac{z-d}{z_0} \right) dz \quad (3)$$

278 given in Bullock et al. (2012) equation 6, with the notation slightly modified. Here, z
 279 is the height above the ground, K is the von Karman constant, and u^* is the friction
 280 velocity. The zero-plane displacement d and roughness length z_0 are surface roughness
 281 parameters that, for a grass canopy height h above the ground, are approximated by
 282 $d \approx 0.7h$ and $z_0 \approx 0.1h$. These estimates are from Raupach (1994) for a canopy area
 283 index $\Lambda = 1$ in which the sum of grass canopy elements is equal to the unit area being
 284 measured. A 0.15 m grass height at the study site gives $d = 0.105$ and z_0 , which are
 285 suitable approximations for grassland (Wiernga, 1993). Calculations of u^* were done
 286 using equation A2 from Skarpaas and Shea (2007), in which

$$287 \quad u^* = KU_m \left[\log \left(\frac{z_m - d}{z_0} \right) \right]^{-1} \quad (4)$$

288 and U_m is the mean wind velocity at the measurement height z_m . Values for the turbulent
 289 flow parameter σ were then calculated using the estimate made by Skarpaas and Shea
 290 (2007) in their equation A4, where

$$291 \quad \sigma = 2A_w^2 \sqrt{\frac{K(z-d)u^*}{C_0U}} \quad (5)$$

292 and C_0 is the Kolmogorov constant. A_w is a constant that relates vertical turbulence
 293 to friction velocity and is approximately equal to 1.3 under the assumptions of above-
 294 canopy flow made by Skarpaas and Shea (2007), based off calculations from Hsieh and
 295 Katul (2005). In addition, the assumption that $z = H$ was made in order to make the
 296 calculation of σ more feasible.

297 The values from the previous three equations give us the necessary information to

298 calculate μ' and λ' , thus allowing us to create the WALD distribution $p(r)$. However, the
 299 base WALD model does not take into account variation in wind speeds or seed terminal
 300 velocities, which limits its applicability in systems where such variation is present. In
 301 order to account for this variation, we integrate the WALD model over distributions these
 302 two variables using the same method as Skarpaas and Shea (2007). The WALD model
 303 assumes seed release from a single point source, though, which is not realistic for a shrub;
 304 because seeds are released across the entire height of the shrub rather than from a point
 305 source, $p(r)$ was also integrated across the uniform distribution from the grass canopy
 306 height to the shrub height. Thus, under the assumptions that the height at which a
 307 seed is located does not affect its probability of being released and that seeds are evenly
 308 distributed throughout the shrub, this gives the dispersal kernel $K(r)$, where

$$309 \quad K(r) = \iiint p(F)p(U)p(z)p(r) dF dU dz \quad (6)$$

310 and $p(F)$ and $p(U)$ are the PDFs of the terminal velocity F and wind speed U , respec-
 311 tively, and $p(z)$ is the uniform distribution from h to H .

312 The distribution $p(F)$ in the integral above was constructed using experimentally
 313 determined seed terminal velocities. This was done by using a high-speed camera and
 314 motion tracking software to determine position as a function of time, and then using the
 315 Levenberg-Marquardt algorithm to solve a quadratic-drag equation of motion for F . Be-
 316 fore seeds were released, they were dried and then dyed with yellow fluorescent powder,
 317 and then put against a black background to improve visibility and make tracking easier.
 318 While the powder added mass to the seeds, this added mass only yielded an approxi-
 319 mately 2.5% increase and was thus negligible, likely having little effect on their terminal
 320 velocities. Measurements were conducted for 48 seeds that were randomly chosen from a
 321 seed pool derived from different plants, and then an empirical PDF of terminal velocities
 322 was constructed using the data. Constructing $p(U)$ involved creating an empirical PDF

of hourly wind speeds at Five Points, the site closest to the 12 transects being used, that were obtained from meteorological data collected at the Sevilleta National Wildlife Refuge from 1988 to 2010. We did not weight $p(U)$ and assumed that the probability seed release from the shrub is the same regardless of wind speed.

Spatial integral projection model

Given that the shrub population at this site is approximately homogeneous perpendicular to the direction of encroachment, expansion is modelled as a wave moving in one dimension. A spatial integral projection model (SIPM) is used to estimate the speed at which encroachment occurs; such a model incorporates the effects of variation in traits like plant size that stage-structured models, such as those described in Neubert and Caswell (2000), do not capture. According to Jonjégans et al. (2011), a general SIPM can be formulated as

$$\mathbf{n}(x_2, z_2, t + 1) = \iint \tilde{K}(x_2, x_1, z_2, z_1) \mathbf{n}(x_1, z_1, t) dx_1 dz_1 \quad (7)$$

where x_1 and x_2 are locations of individuals of a particular size before and after one unit of time, and z_1 and z_2 are the respective sizes. The vector \mathbf{n} indicates the population density of each size, and \tilde{K} is a kernel that combines dispersal with demography. Though this SIPM represents a continuous spectrum of shrub sizes and densities, it was implemented by discretising the above integral with a 200 x 200 matrix, as this makes calculations significantly more tractable.

Movement of the wave is determined by the components of the combined dispersal-demography kernel \tilde{K} , which is of the same form as that used in Jonjégans et al. (2011). Here,

$$\tilde{K}(x_2, x_1, z_2, z_1) = K(x_2 - x_1)Q(z_2 - z_1) + \delta(x_2 - x_1)G(z_2 - z_1) \quad (8)$$

and K is the dispersal kernel, Q a reproduction function, G a growth function, and δ

the Dirac delta function. G is derived from the model for annual growth ratio, and Q is derived from the reproductive structures model as well as other factors including number of seeds per reproductive structure, probability of recruitment from seed, and recruit size. Both G and Q give the probability of transition between sizes; in the case of G , this is the probability of growing from one specific size to another, and in the case of Q the probability that an individual of a specific size produces a recruit of a specific size. The product of K and Q represents the production and dispersal of motile propagules, while the product of G and δ represents the growth of sessile individuals.

Given growth function G and the reproduction function Q , the speed of the moving wave can be calculated as

$$c^* = \min_{s>0} \left[\frac{1}{s} \ln(\rho_s) \right] \quad (9)$$

where s is the wave shape parameter and ρ_s is the dominant eigenvalue of the kernel \mathbf{H}_s (Jongejans et al., 2011). This estimate for the wavespeed is valid under the assumption that population growth decreases monotonically as conspecific density increases, with the highest rates of growth occurring at the lowest population densities (Lewis et al., 2006). The kernel \mathbf{H}_s is defined as

$$\mathbf{H}_s = M(s)Q(z_2 - z_1) + G(z_2 - z_1) \quad (10)$$

where $M(s)$ is the moment-generating function of the dispersal kernel (Jongejans et al., 2011). For one-dimensional dispersal, this moment-generating function can be estimated as

$$M(s) = \frac{1}{N} \sum_{i=1}^n I_0(sr_i) \quad (11)$$

where r is the dispersal distance for each observation, and I_0 is the modified Bessel function of the first kind and zeroth order (Skarpaas and Shea, 2007). In order to obtain M , numerous dispersal distances were simulated from the dispersal kernel $K(r)$ described

in the previous section, with over 2000 replications for each shrub height increment of 1 cm. This was performed over the range from the lowest possible dispersal height to the maximum shrub height. Once $M(s)$ was obtained for dispersal at each shrub height, \mathbf{H}_s and c^* were calculated for each value of s ; this was done for values of s ranging from 0 to 2, as it is this range in which c^* occurs.

Results

Encroachment re-surveys

Figure 1.

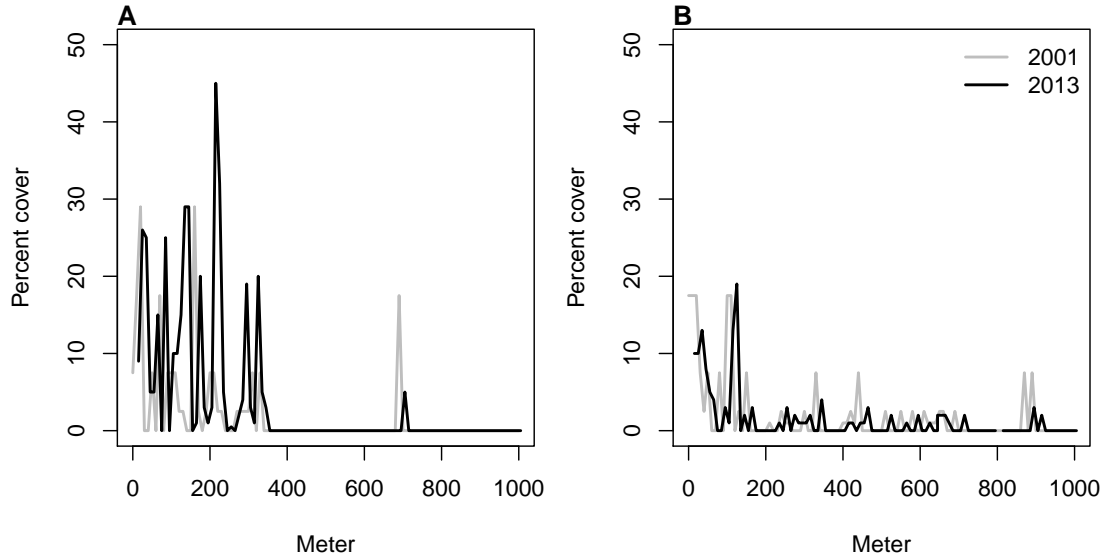


Figure 1: Re-surveys of shrub cover along two permanent transects (A,B) surveyed in 2001 and 2013.

The speed of encroachment at the study site as estimated by the SIPM is rather slow; as can be seen in Figure 2, the low-density wavefront moves at approximately 0.5 cm/yr under normal conditions and at 1 cm/yr under the best seedling survival conditions observed in the dataset. These improved conditions were observed due to above-average rainfall that occurred after greenhouse-grown seedlings were transplanted

384 to the site. Population growth in this low-density region of the moving wave is also low,
 385 with a geometric growth rate of $\lambda \approx 1.006$ and even lower rates of growth the higher-
 386 density regions behind; in the higher-survival scenario the maximum rate increases to
 387 $\lambda \approx 1.013$, with growth still decreasing as density increases. For both scenarios, the
 388 decrease in population growth rate with increasing density was monotonic across the
 389 range of observed standardised densities, as is shown in Figure 2. This suggests that
 390 an Allee effect is likely not present in this population, as the highest rate of population
 391 growth is found at the lowest density vanguard of the encroaching population. Thus, the
 392 conditions necessary for equation 9 to be valid are satisfied, and these wavespeeds are
 393 applicable for a pulled-wave scenario in which no Allee effects are present.

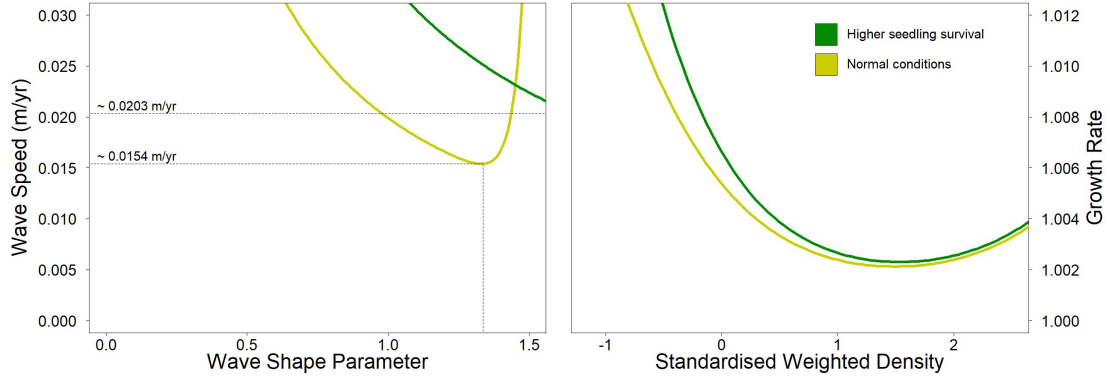


Figure 2: Estimated encroachment wave speeds (left) and geometric rates of population growth (right) for higher post-rainfall seedling survival and normal conditions.

394 As the speed of encroachment is quite limited, so is the extent of wind dispersal.
 395 Long distance dispersal events, while more common for taller shrubs than their shorter
 396 counterparts, are still uncommon overall. For the tallest shrub height of 1.98 m, only
 397 0.32% of propagules exceed a dispersal distance of 5 m, and 0.02% exceed 10 m. At 1
 398 m, or approximately half the tallest shrub height, long distance dispersal is even less
 399 likely, with 0.0046% of propagules exceeding a dispersal distance of 5 m and 0.0009%
 400 exceeding 10 m. Given that the median shrub height is only 0.64 m, the occurrence of

401 long-distance wind dispersal in most of the shrub population is highly improbable, and
402 the few instances in which it occurs will only be limited to the tallest shrubs. Thus, as
403 Figure 3 demonstrates, shorter dispersal distances dominate; even for the tallest shrub,
404 81% of seeds fall within only a metre of the plant, and this percentage increases as
405 shrub height decreases. Dispersal kernels have their highest probability density at dis-
406 persal distances between 2 and 8 cm from the shrub; here, as shrub height increases, the
407 most probable dispersal distance slightly increases while maximum probability density
408 decreases. Regardless of the shrub height, most dispersal will occur very close to the
409 plant, though increases in shrub height dramatically increase the likelihood of dispersal
410 at longer distances. It is clear that the shape of the height-dependent dispersal kernel
411 $K(r)$ varies greatly among the shrub population given the large range of shrub heights
412 observed; shrubs at lower heights have more slender kernels with most of the seeds dis-
413 persing closer to the plant, while taller shrubs have kernels with much fatter tails and
414 are more capable of longer-distance dispersal.

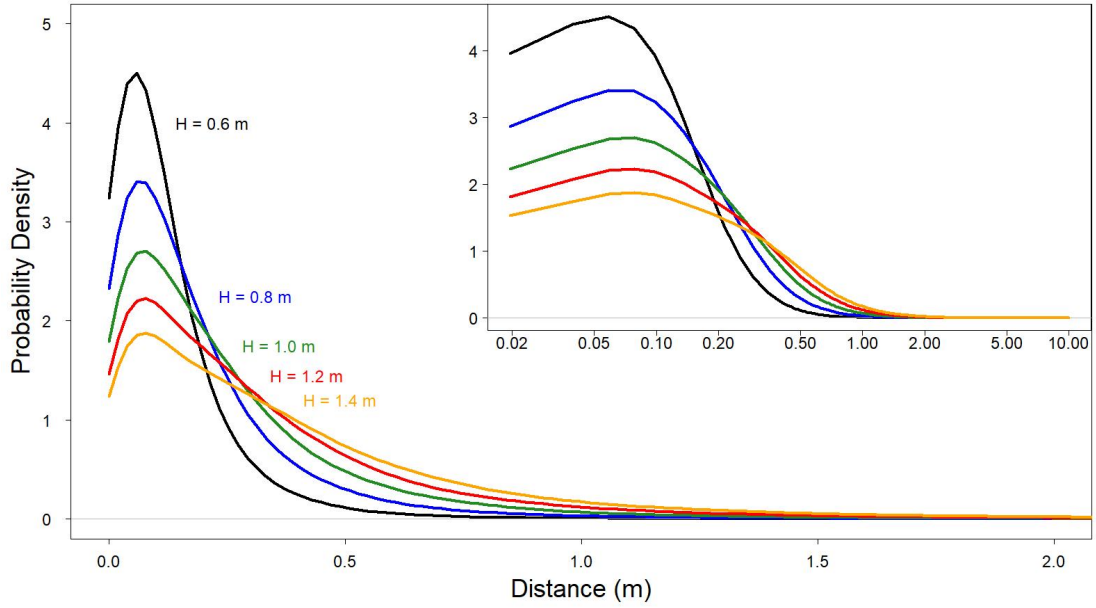


Figure 3: Dispersal kernels, with each colour representing a selected shrub height. The inset plot is the same as the large plot, though with a logarithmic x-axis to more easily show differences in dispersal probability at smaller distances.

415 Density and size dependence are evident in all 4 of the demographic rates, with
 416 coefficients for each model displayed in Table 2. For growth, reproduction, and survival,
 417 density dependence is mostly negative and monotonic; this is not the case for probability
 418 of flowering, where shrub size seems to be more important than the effects of density alone
 419 and suggests that larger shrubs have a higher probability of flowering than their smaller
 420 counterparts. This, along with size and density dependence in growth and reproduction,
 421 is shown in Figure 4. Size dependence is positive for reproduction, as would be expected
 422 since larger plants typically produce more flowers and fruits. However, annual growth
 423 decreases as size increases; this could be in part due to the annual growth in this study
 424 being quantified as a proportion relative to the shrub's initial size. While larger shrubs
 425 may produce more plant material over a year in terms of absolute volume, smaller shrubs
 426 produce less but can still have higher annual growth in terms of the percentage of volume

427 added relative to their initial volume. When compared to density, shrub size is a much
428 stronger predictor of survival, with significant differences in mortality rates depending on
429 shrub size. For small shrubs, mortality is exceptionally high, and increases in volume for
430 these shrubs only slightly increase the likelihood of survival. However, after shrubs reach
431 a logarithmic volume of approximately 7.3, they are almost guaranteed to survive, with
432 survival rates near 100% persisting regardless of any further size increases. Interestingly,
433 though most recruits were found at lower densities, the probability of recruitment from
434 seed displays positive density dependence; the probability of recruitment was still very
435 low, though, with a baseline rate of approximately 2 recruits per 10,000 seeds.

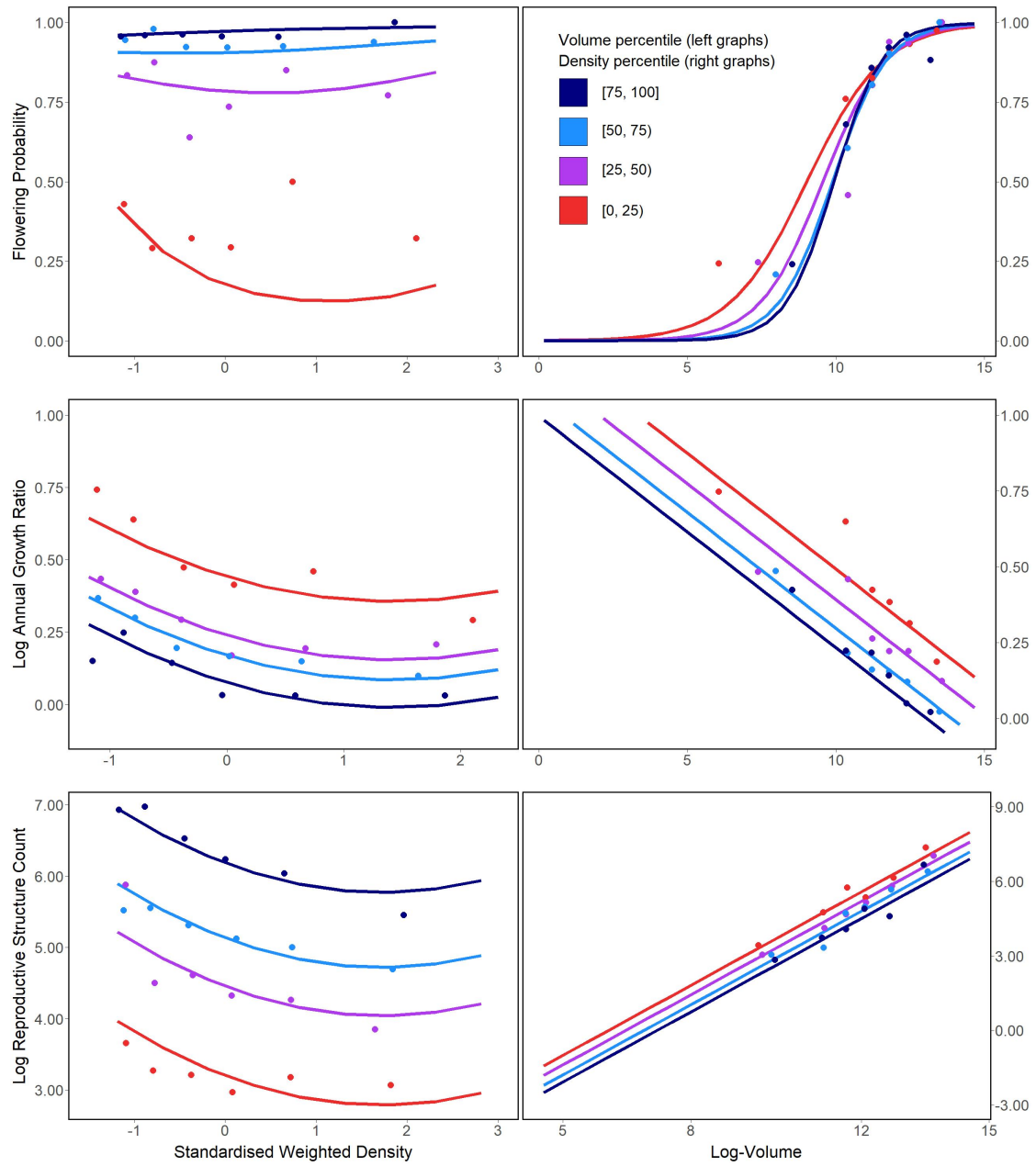


Figure 4: Flowering probability (top row), log annual growth ratio (centre row), and log reproductive structure count (bottom row) at all four sampling sites. In the left column of graphs, the three response variables are shown as a function of density for each of four volume quartiles, with each quartile containing six density bins; in the right column, the opposite occurs, with response variables shown as functions of four volume quartiles that each contain six density bins. Graphs quantifying the number of reproductive structures include data only on plants that flowered.

Discussion

The slow movement of the encroaching creosotebush wave at the Sevilleta LTER site can likely be contributed to a combination of three factors: short dispersal distances with extremely limited long-distance dispersal events, very low probability of recruitment from seed, and high seedling mortality. These three barriers, when combined, form a formidable challenge to the establishment of new shrubs at the low-density front of the wave. First, a seed must travel far enough to avoid competition with the parent shrub, which is unlikely given the dispersal kernels shown in Figure 2. Even if the seed manages to be dispersed this far, its chances of becoming a seedling are low. Caching and consumption by seed-eaters such as a variety of seed-harvesting ants (Whitford, 1978; Whitford et al., 1980; Lei, 1999) and the kangaroo rat *Dipodomys merriami* (Chew and Chew, 1970) decreases the amount of seeds available for germination. However, reduction in germination caused by destruction of seeds may be partly mitigated by the more favourable germination conditions that these seeds can experience when cached underground (Chew and Chew, 1970). Many of the remaining seeds will still fail to germinate, and in the unlikely event that germination does occur, seedlings will likely die given the high rates of mortality observed in smaller shrubs. Such high rates of creosotebush seedling mortality have been observed in other studies as well (Boyd and Brum, 1983; Bowers et al., 2004), probably due to a combination of herbivory, competition, and abiotic stresses.

However, as low as they are, the wavespeed estimates given in this paper are still conservative estimates for reasons mostly related to dispersal. First, it is important to note that the dispersal kernels used here, while they account for variation in factors such as wind speed and terminal velocity, may underestimate the distances that shrub propagules travel. Because the WALD model assumes that terminal velocity is reached immediately upon seed release, seeds in the estimate thus take a shorter time to fall

462 and have less time to be transported by wind, and the true frequency of long-distance
463 dispersal events may thus be greater than what is estimated here. Second, dispersal at the
464 study site could occur through additional mechanisms other than wind. For example,
465 secondary dispersal through runoff from significant rainfall events can transport seeds
466 (Thompson et al., 2014), and given that long-distance dispersal by bird and subsequent
467 species divergence is thought to be responsible for creosotebush being in North America
468 in the first place (Wells and Hunziker, 1976), short-distance dispersal by other animals
469 at the study site likely occurs. As mentioned above, seeds are transported by seed-
470 harvesting ants and granivorous mammals, where they are often stored in caches that
471 can be appreciable distances from the parent shrubs. Whether transportation occurs via
472 ant or rodent, creosotebush seeds can be moved significantly further than wind alone
473 can, though many of these seeds are eventually consumed.

474 Despite the more conservative estimates our model yields, the estimated rate of dis-
475 persal in creosotebush populations at the Sevilleta National Wildlife Refuge is consistent
476 with observations from the past 50-60 years, as creosotebush expansion during this time
477 has been minimal (Moreno-de las Heras et al., 2016). However, it cannot explain the
478 long-term increases in creosotebush cover at the study site, as total encroachment over
479 the past 150 years is much greater than what would be expected given the encroachment
480 rates derived by our models. Such a discrepancy is likely due to much of the expansion
481 occurring in an episodic fashion, with short times during which rapid encroachment oc-
482 curs due to favourable environmental conditions. This could be due in part to seedling
483 recruitment, which is a factor that strongly limits creosotebush expansion, being rare
484 and episodic. For example, Allen et al. (2008) estimate that a major recruitment event
485 occurred at this site in the 1950s, which is supported by photographic evidence from
486 Milne et al. (2003) of a drought-driven expansion during this time. Moreno-de las Heras
487 et al. (2016) estimate that after this expansion, several smaller creosotebush recruitment
488 events occurred in decadal episodes. However, such events can be highly localised and

489 may not necessarily occur at the low-density front of encroachment, which could explain
490 how these recruitment events can still coexist with lack of encroachment in the recent
491 past.

492 Overall, our observations and model highlight three aspects of creosotebush encroach-
493 ment that should be the focus of future studies seeking to obtain better estimates of
494 encroachment rates. First, negative density dependence in survival, growth, and repro-
495 duction is demonstrated, along with size dependence. The clear dependence on size and
496 conspecific density suggests that they both should be considered when estimating cre-
497 osotebush expansion and quantifying the demographic variation that contributes to it.
498 Second, wind dispersal in these shrubs is quite limited; though the dispersal kernels seen
499 here are typical in the sense that they are characterised by high near-plant dispersal and
500 exceptionally low long-distance dispersal, the scale across which such dispersal occurs
501 is small, with most seeds landing within only 1 m of the shrub. Wind dispersal alone
502 may be an underestimate of the true amount of dispersal occurring, and future work
503 should seek to incorporate the effects of dispersal by runoff and animals so that a more
504 representative model of total dispersal can be obtained. Finally, encroachment is slow or
505 even stagnates, but only most of the time. Though our encroachment speed estimates
506 are representative of creosotebush populations for most years, the significant expansion
507 seen over larger time scales suggests that there is episodic expansion in other years; while
508 our model is consistent with the recent stagnation in creosotebush encroachment at the
509 Sevilleta LTER site, a model that also includes interannual variability in factors such
510 as survival and recruitment would be able to better account for instances of episodic
511 population expansion that are characteristic of this location.

512 Acknowledgements

513 Author contributions

514 Data accessibility

515 References

- 516 Bowers, J. E., R. M. Turner, and T. L. Burgess. 2004. Temporal and spatial patterns in
517 emergence and early survival of perennial plants in the Sonoran Desert. *Plant Ecology*
518 **172**:107–119.
- 519 Boyd, R. S., and G. D. Brum. 1983. Postdispersal reproductive biology of a Mojave Desert
520 population of *Larrea tridentata* (Zygophyllaceae). *American Midland Naturalist* pages
521 25–36.
- 522 Brandt, J. S., M. A. Haynes, T. Kuemmerle, D. M. Waller, and V. C. Radeloff. 2013.
523 Regime shift on the roof of the world: Alpine meadows converting to shrublands in
524 the southern Himalayas. *Biological Conservation* **158**:116–127.
- 525 Buffington, L. C., and C. H. Herbel. 1965. Vegetational changes on a semidesert grassland
526 range from 1858 to 1963. *Ecological monographs* **35**:139–164.
- 527 Cabral, A., J. De Miguel, A. Rescia, M. Schmitz, and F. Pineda. 2003. Shrub encroach-
528 ment in Argentinean savannas. *Journal of Vegetation Science* **14**:145–152.
- 529 Chen, L., H. Li, P. Zhang, X. Zhao, L. Zhou, T. Liu, H. Hu, Y. Bai, H. Shen, and J. Fang.
530 2015. Climate and native grassland vegetation as drivers of the community structures
531 of shrub-encroached grasslands in Inner Mongolia, China. *Landscape Ecology* **30**:1627–
532 1641.

533 Chew, R. M., and A. E. Chew. 1970. Energy relationships of the mammals of a desert
534 shrub (*Larrea tridentata*) community. *Ecological Monographs* pages 2–21.

535 D’Odorico, P., J. D. Fuentes, W. T. Pockman, S. L. Collins, Y. He, J. S. Medeiros,
536 S. DeWekker, and M. E. Litvak. 2010. Positive feedback between microclimate and
537 shrub encroachment in the northern Chihuahuan desert. *Ecosphere* **1**:1–11.

538 D’Odorico, P., G. S. Okin, and B. T. Bestelmeyer. 2012. A synthetic review of feedbacks
539 and drivers of shrub encroachment in arid grasslands. *Ecohydrology* **5**:520–530.

540 Gardner, J. L. 1951. Vegetation of the creosotebush area of the Rio Grande Valley in
541 New Mexico. *Ecological Monographs* **21**:379–403.

542 Gibbens, R., R. McNeely, K. Havstad, R. Beck, and B. Nolen. 2005. Vegetation changes
543 in the Jornada Basin from 1858 to 1998. *Journal of Arid Environments* **61**:651–668.

544 Goslee, S., K. Havstad, D. Peters, A. Rango, and W. Schlesinger. 2003. High-resolution
545 images reveal rate and pattern of shrub encroachment over six decades in New Mexico,
546 USA. *Journal of Arid Environments* **54**:755–767.

547 Grover, H. D., and H. B. Musick. 1990. Shrubland encroachment in southern New Mexico,
548 USA: an analysis of desertification processes in the American Southwest. *Climatic*
549 *change* **17**:305–330.

550 Hanzawa, F. M., and S. Kalisz. 1993. The relationship between age, size, and reproduc-
551 tion in *Trillium grandiflorum* (Liliaceae). *American Journal of Botany* **80**:405–410.

552 HARA, T. 1993. Mode of competition and size-structure dynamics in plant communities.
553 *Plant Species Biology* **8**:75–84.

554 Jongejans, E., K. Shea, O. Skarpaas, D. Kelly, and S. P. Ellner. 2011. Importance of
555 individual and environmental variation for invasive species spread: a spatial integral
556 projection model. *Ecology* **92**:86–97.

557 Katul, G., A. Porporato, R. Nathan, M. Siqueira, M. Soons, D. Poggi, H. Horn, and
 558 S. A. Levin. 2005. Mechanistic analytical models for long-distance seed dispersal by
 559 wind. *The American Naturalist* **166**:368–381.

560 Keitt, T. H., M. A. Lewis, and R. D. Holt. 2001. Allee effects, invasion pinning, and
 561 species' borders. *The American Naturalist* **157**:203–216.

562 Kelleway, J. J., K. Cavanaugh, K. Rogers, I. C. Feller, E. Ens, C. Doughty, and N. Sain-
 563 tilan. 2017. Review of the ecosystem service implications of mangrove encroachment
 564 into salt marshes. *Global Change Biology* **23**:3967–3983.

565 Knapp, A. K., J. M. Briggs, S. L. Collins, S. R. Archer, M. S. BRET-HARTE, B. E.
 566 Ewers, D. P. Peters, D. R. Young, G. R. Shaver, E. Pendall, et al. 2008. Shrub
 567 encroachment in North American grasslands: shifts in growth form dominance rapidly
 568 alters control of ecosystem carbon inputs. *Global Change Biology* **14**:615–623.

569 Kot, M., M. A. Lewis, and P. van den Driessche. 1996. Dispersal data and the spread of
 570 invading organisms. *Ecology* **77**:2027–2042.

571 Lei, S. A. 1999. Ecological impacts of *Pogonomyrmex* on woody vegetation of a *Larrea*-
 572 *Ambrosia* shrubland. *The Great Basin Naturalist* pages 281–284.

573 Lewis, M., and P. Kareiva. 1993. Allee dynamics and the spread of invading organisms.
 574 *Theoretical Population Biology* **43**:141–158.

575 Lewis, M. A., M. G. Neubert, H. Caswell, J. S. Clark, and K. Shea, 2006. A guide
 576 to calculating discrete-time invasion rates from data. Pages 169–192 *in* *Conceptual*
 577 *ecology and invasion biology: reciprocal approaches to nature*. Springer.

578 Moreno-de las Heras, M., L. Turnbull, and J. Wainwright. 2016. Seed-bank structure
 579 and plant-recruitment conditions regulate the dynamics of a grassland-shrubland Chi-
 580 huahuan ecotone. *Ecology* **97**:2303–2318.

- 581 Mugasi, S., E. Sabiiti, and B. Tayebwa. 2000. The economic implications of bush
582 encroachment on livestock farming in rangelands of Uganda. *African Journal of Range*
583 *and Forage Science* **17**:64–69.
- 584 Nathan, R., G. G. Katul, G. Bohrer, A. Kuparinen, M. B. Soons, S. E. Thompson,
585 A. Trakhtenbrot, and H. S. Horn. 2011. Mechanistic models of seed dispersal by wind.
586 *Theoretical Ecology* **4**:113–132.
- 587 Neubert, M. G., and H. Caswell. 2000. Demography and dispersal: calculation and
588 sensitivity analysis of invasion speed for structured populations. *Ecology* **81**:1613–
589 1628.
- 590 Oba, G., E. Post, P. Syvertsen, and N. Stenseth. 2000. Bush cover and range condition
591 assessments in relation to landscape and grazing in southern Ethiopia. *Landscape*
592 *ecology* **15**:535–546.
- 593 Pan, S., and G. Lin. 2012. Invasion traveling wave solutions of a competitive system
594 with dispersal. *Boundary Value Problems* **2012**:120.
- 595 Parizek, B., C. M. Rostagno, and R. Sottini. 2002. Soil erosion as affected by shrub
596 encroachment in northeastern Patagonia. *Rangeland Ecology & Management/Journal*
597 *of Range Management Archives* **55**:43–48.
- 598 Peng, H.-Y., X.-Y. Li, G.-Y. Li, Z.-H. Zhang, S.-Y. Zhang, L. Li, G.-Q. Zhao, Z.-Y. Jiang,
599 and Y.-J. Ma. 2013. Shrub encroachment with increasing anthropogenic disturbance
600 in the semiarid Inner Mongolian grasslands of China. *Catena* **109**:39–48.
- 601 PICKERING, C. M. 1994. Size-dependent reproduction in Australian alpine *Ranunculus*.
602 *Australian journal of ecology* **19**:336–344.
- 603 Ratajczak, Z., J. B. Nippert, and S. L. Collins. 2012. Woody encroachment decreases
604 diversity across North American grasslands and savannas. *Ecology* **93**:697–703.

605 Ravi, S., P. D’Odorico, S. L. Collins, and T. E. Huxman. 2009. Can biological invasions
606 induce desertification? *The New Phytologist* **181**:512–515.

607 Reed, M., L. Stringer, A. Dougill, J. Perkins, J. Atlhopheng, K. Mulale, and N. Favretto.
608 2015. Reorienting land degradation towards sustainable land management: Linking
609 sustainable livelihoods with ecosystem services in rangeland systems. *Journal of envi-
610 ronmental management* **151**:472–485.

611 Roques, K., T. O’connor, and A. R. Watkinson. 2001. Dynamics of shrub encroach-
612 ment in an African savanna: relative influences of fire, herbivory, rainfall and density
613 dependence. *Journal of Applied Ecology* **38**:268–280.

614 Schlesinger, W. H., and A. M. Pilmanis. 1998. Plant-soil interactions in deserts. *Biogeo-
615 chemistry* **42**:169–187.

616 Schlesinger, W. H., J. F. Reynolds, G. L. Cunningham, L. F. Huenneke, W. M. Jarrell,
617 R. A. Virginia, and W. G. Whitford. 1990. Biological feedbacks in global desertification.
618 *Science* **247**:1043–1048.

619 Sirami, C., and A. Monadjem. 2012. Changes in bird communities in Swaziland savannas
620 between 1998 and 2008 owing to shrub encroachment. *Diversity and Distributions*
621 **18**:390–400.

622 Skarpaas, O., and K. Shea. 2007. Dispersal patterns, dispersal mechanisms, and invasion
623 wave speeds for invasive thistles. *The American Naturalist* **170**:421–430.

624 Smith, G. R., H. A. Dingfelder, and D. A. Vaala. 2003. Effect of plant size and density
625 on garlic mustard reproduction. *Northeastern Naturalist* **10**:269–276.

626 Sullivan, L. L., B. Li, T. E. Miller, M. G. Neubert, and A. K. Shaw. 2017. Density depen-
627 dence in demography and dispersal generates fluctuating invasion speeds. *Proceedings
628 of the National Academy of Sciences* **114**:5053–5058.

- 629 Taylor, C. M., and A. Hastings. 2005. Allee effects in biological invasions. *Ecology*
630 *Letters* **8**:895–908.
- 631 Thompson, S. E., S. Assouline, L. Chen, A. Trahktenbrot, T. Svoray, and G. G. Katul.
632 2014. Secondary dispersal driven by overland flow in drylands: Review and mechanistic
633 model development. *Movement ecology* **2**:7.
- 634 Trollope, W., F. Hobson, J. Danckwerts, and J. Van Niekerk. 1989. Encroachment and
635 control of undesirable plants. *Veld management in the Eastern Cape* pages 73–89.
- 636 Turnbull, L., J. Wainwright, and R. E. Brazier. 2010. Changes in hydrology and erosion
637 over a transition from grassland to shrubland. *Hydrological Processes: An Interna-*
638 *tional Journal* **24**:393–414.
- 639 Van Auken, O. 2009. Causes and consequences of woody plant encroachment into western
640 North American grasslands. *Journal of environmental management* **90**:2931–2942.
- 641 Van Auken, O. W. 2000. Shrub invasions of North American semiarid grasslands. *Annual*
642 *review of ecology and systematics* **31**:197–215.
- 643 Veit, R. R., and M. A. Lewis. 1996. Dispersal, population growth, and the Allee ef-
644 fect: dynamics of the house finch invasion of eastern North America. *The American*
645 *Naturalist* **148**:255–274.
- 646 Wang, M.-H., M. Kot, and M. G. Neubert. 2002. Integrodifference equations, Allee
647 effects, and invasions. *Journal of mathematical biology* **44**:150–168.
- 648 Weiner, J. 1990. Asymmetric competition in plant populations. *Trends in ecology &*
649 *evolution* **5**:360–364.
- 650 Wells, P. V., and J. H. Hunziker. 1976. Origin of the creosote bush (*Larrea*) deserts of
651 southwestern North America. *Annals of the Missouri Botanical Garden* pages 843–861.

- 652 Whitford, W., E. Depree, and P. Johnson. 1980. Foraging ecology of two chihuahuan
653 desert ant species: *Novomessor cockerelli* and *Novomessor albisetosus*. *Insectes Sociaux*
654 **27**:148–156.
- 655 Whitford, W. G. 1978. Structure and seasonal activity of Chihuahua desert ant commu-
656 nities. *Insectes Sociaux* **25**:79–88.
- 657 Wiernga, J. 1993. Representative roughness parameters for homogeneous terrain.
658 *Boundary-Layer Meteorology* **63**:323–363.